

Dopaminergic Modulation of Synaptic Integration and Firing Patterns in the Rat Entopeduncular Nucleus

Hagar Lavian,¹ Mara Almog,² Ravit Madar,^{1,2,3} Yocheved Loewenstern,¹ Izhar Bar-Gad,¹ Eitan Okun,^{1,2,3} and Alon Korngreen^{1,2}

¹The Leslie and Susan Gonda Interdisciplinary Brain Research Center, ²The Mina and Everard Goodman Faculty of Life Sciences, and ³The Paul Feder Laboratory on Alzheimer's disease research, Bar Ilan University, Ramat Gan 52900, Israel

Dopamine is known to differentially modulate the impact of cortical input to the striatum between the direct and indirect pathways of the basal ganglia (BG). However, the role of extrastriatal dopamine receptors (DRs) in BG information processing is less clear. To investigate the role of extrastriatal DRs, we studied their distribution and function in one of the output nuclei of the BG of the rodent, the entopeduncular nucleus (EP). qRT-PCR indicated that all DR subtypes were expressed by EP neurons, suggesting that both D₁-like receptors (D1LRs) and D₂-like receptors (D2LRs) were likely to affect information processing in the EP. Whole-cell recordings revealed that striatal inputs to the EP were potentiated by D1LRs whereas pallidal inputs to the EP were depressed by D2LRs. Changes to the paired-pulse ratio of inputs to the EP suggested that dopaminergic modulation of striatal inputs is mediated by postsynaptic receptors, and that of globus pallidus-evoked inputs is mediated by presynaptic receptors. We show that these changes in synaptic efficacy changed the information content of EP neuron firing. Overall, the findings suggest that the dopaminergic system affects the passage of feedforward information through the BG by modulating input divergence in the striatum and output convergence in the EP.

Key words: basal ganglia; dopamine; entopeduncular; entropy; GABA; patch clamp; plasticity

Significance Statement

The entopeduncular nucleus (EP), one of the basal ganglia (BG) output nuclei, is an important station in information processing in BG. However, it remains unclear how EP neurons encode information and how dopamine affects this process. This contrasts with the well established role of dopamine in the striatum, which is known to redistribute cortical input between the direct and indirect pathways. Here we show that, in symmetry with the striatum, dopamine controls the rebalancing of information flow between the two pathways in the EP. Specifically, we demonstrate that dopamine regulates EP activity by differentially modulating striatal and pallidal GABAergic inputs. These results call for a reassessment of current perspectives on BG information processing by highlighting the functional role of extrastriatal dopamine receptors.

Introduction

The classic model of the basal ganglia (BG) posits that dopaminergic modulation of the input stage of these nuclei (cortico-striatal transmission) is responsible for balancing the information

flow between the direct and indirect pathways (Gerfen and Surmeier, 2011), which leads to the modulation of learning, reward signaling, and the execution of motor actions (Beninger, 1983; Schultz et al., 1992; Nakahara et al., 2004; Wickens et al., 2007). However, dopaminergic innervation and dopamine receptors (DRs) are present in many other structures of the basal ganglia, such as the globus pallidus (GP), the substantia nigra pars reticulata (SNr), and the entopeduncular nucleus (EP; Lindvall et al., 1974; Beckstead et al., 1979; Yung et al., 1995; Rivera et al., 2003; Fuchs and Hauber, 2004; Kliem et al., 2010; Mitkovski et al., 2012). Nigral dopaminergic axons innervating the striatum (STR) form collaterals in the EP and GP (Smith et al., 1989; Caillé et al., 1996; Gauthier et al., 1999; Bolam et al., 2000; Watabe-Uchida et al., 2012), thus suggesting a concurrent modulation of multiple basal ganglia nuclei by the same neurons. However, the role of dopamine in shaping extrastriatal integration and conse-

Received March 7, 2017; revised June 7, 2017; accepted June 13, 2017.

Author contributions: H.L., M.A., R.M., Y.L., I.B.-G., E.O., and A.K. designed research; H.L., M.A., R.M., Y.L., I.B.-G., E.O., and A.K. performed research; H.L., M.A., R.M., Y.L., I.B.-G., E.O., and A.K. analyzed data; H.L., Y.L., I.B.-G., E.O., and A.K. wrote the paper.

This work was supported by a grant from the Israel Science Foundation—Heritage Biomedical Science Partnership program of the Israel Science Foundation to AK and IBG (Grant 138/15), and a Paul Feder Foundation for Neurodegenerative Disorder Research grant to E.O.

The authors declare no competing financial interests.

Correspondence should be addressed to Dr. Alon Korngreen, Bar Ilan University, The Leslie and Susan Gonda Interdisciplinary Brain Research Center, The Mina and Everard Goodman Faculty of Life Sciences, Ramat Gan 52900, Israel. E-mail: alon.korngreen@biu.ac.il.

DOI:10.1523/JNEUROSCI.0639-17.2017

Copyright © 2017 the authors 0270-6474/17/377177-11\$15.00/0

quently the output of the basal ganglia remains unclear (Romelfanger and Wichmann, 2010).

The EP, the rodent equivalent of the primate GP internal segment, a major output nucleus of the BG, is a key structure in the process of action selection. Dendrites of single EP neurons are innervated by GABAergic axons of striatal spiny projection neurons (SPNs), whereas the soma of these neurons is innervated by GABAergic axons arriving from the GP (Nagy et al., 1978; Bolam and Smith, 1992). Thus, individual EP neurons directly process information stemming from both the direct and indirect pathways. Functionally, the GABA concentration in the EP is affected by dopaminergic agonists and antagonists (Floran et al., 1990; Aceves et al., 1995; Kliem et al., 2007). Following dopamine depletion, the firing rate, firing pattern, and entropy rate of EP neurons change (DeLong, 1990; Filion and Tremblay, 1991; Ruskin et al., 2002; Darbin et al., 2016). Anatomically, the EP is a bottleneck for information flow in the basal ganglia (Bar-Gad et al., 2000). In rats, the striatum consists of 2.8 million neurons, the GP consists of 45,000 neurons, whereas the EP consists of only 3000 neurons (Oorschot, 1996). This extensive anatomical reduction through BG stations is a clear indication that feedforward information from the cortex is subjected to massive reduction that leads to a highly compact representation of cortical information before being expanded back to the cortex via the thalamus (Bergman et al., 1998). This funnel-like structure accounts for the large global impact of any modulation of information at the EP bottleneck.

Based on these converging anatomical, theoretical, and functional findings, we hypothesized that dopamine plays a key role in the convergence of the pathways into the EP in addition to its role in their divergence from the striatum. Here we tested this hypothesis using quantitative real-time PCR (qRT-PCR), whole-cell patch-clamp recordings, and numerical modeling.

Materials and Methods

Animals. All procedures were approved and supervised by the Institutional Animal Care and Use Committee and were in accordance with the National Institutes of Health *Guide for the Care and Use of Laboratory Animals* and the Bar-Ilan University Guidelines for the Use and Care of Laboratory Animals in Research. This study was approved by the Israel National Committee for Experiments in Laboratory Animals at the Ministry of Health.

Quantitative real-time PCR to assess mRNA expression levels of dopamine receptors. Five adult female Wistar rats were used for qRT-PCR. Rats were anesthetized using isoflurane, followed by an intramuscular injection of ketamine HCl (100 mg/kg) and xylazine HCl (10 mg/kg). Rats were killed by rapid decapitation, the brain was quickly removed, and sagittal slices (400 μ m) were cut on an HM 650 V Slicer (MICROM International). The EP or STR was mechanically isolated from the slice, frozen on dry ice, and stored at -80°C until use. RNA was extracted from either the striatum or EP using a TRIzol Reagent (Ambion, Life Technologies). cDNA was generated using the RevertAid H Minus First Strand cDNA Synthesis Kit (Thermo Fisher Scientific). RT-PCR reactions were performed using Fast SYBR Green Master Mix (Applied Biosystems) in a StepOnePlus instrument (Applied Biosystems). Primers were calibrated, and a negative control was performed for each primer pair. Samples were measured in triplicate, and values were normalized to mRNA levels of β -actin. Denaturing was performed at 94°C for 30 s, annealing was performed for 10 s (the temperature for each primer pair is indicated in Table 1), and elongation was performed at 72°C for 10 s. Quantification was assessed at the logarithmic phase of the PCR using the $2^{-\Delta\Delta\text{CT}}$ method.

In vitro slice preparation. Brain slices were obtained from 15- to 21-day-old Wistar rats as previously described (Stuart et al., 1993; Lavian et al., 2013). Rats were killed by rapid decapitation following the guidelines of

Table 1. Primers used for quantitative real-time PCR to assess mRNA expression of the five subtypes of dopamine receptors and β -actin

Gene	Annealing temperature	Accession number	Product length (bp)	Primer sequences
DRD1	55°C	NM_012546.3	168	Forward: 5'-TCCTTCAAGAGGGAGACGAA-3' Reverse: 5'-CCACACAACACATCGAAGG-3'
DRD2	58°C	NM_012547.1	230	Forward: 5'-CATTGTCTGGTCTGTCT-3' Reverse: 5'-GCTCTGAAAGCTCGACTGCT-3'
DRD3	59°C	NM_017140.2	104	Forward: 5'-GAGCTCTGTAGACGTGTGG-3' Reverse: 5'-TGGGATCCCCGTGTGTG-3'
DRD4	56°C	NM_012944.2	166	Forward: 5'-GTAGTGGGGCCTCTCTGTA-3' Reverse: 5'-CGGCATTGAAGATGGTGTAG-3'
DRD5	58°C	NM_012768.1	146	Forward: 5'-GTATCATCAGCGTGGACCGT-3' Reverse: 5'-CAAATTGAGTTGGACCGGGA-3'
Actin	56°C	NM_031144.3	165	Forward: 5'-TGTCACCAACTGGGACGATA-3' Reverse: 5'-GGGGTGTGAAGTCTCAAA-3'

the Bar-Ilan University Animal Welfare Committee. The brain was quickly removed and placed in ice-cold artificial CSF (ACSF) containing the following (in mM): 125 NaCl, 2.5KCl, 15 NaHCO₃, 1.25 Na₂HPO₄, 2 CaCl₂, 1 MgCl₂, 25 glucose, and 0.5 Na-ascorbate, pH 7.4 with 95% O₂/5%CO₂. In all experiments, the ACSF solution contained APV (50 μ M) and CNQX (15 μ M) to block NMDA and AMPA receptors, respectively. Thick sagittal slices (320–370 μ m) were cut at an angle of 17° to the midline on an HM 650 V Slicer (MICROM International) and transferred to a submersion-type chamber, where they were maintained for the remainder of the day in ACSF at room temperature. Experiments were performed at 37°C , and the recording chamber was constantly perfused with oxygenated ACSF. We observed functional connectivity among the striatum, GP, and EP only when the brain was sliced at $\sim 17^{\circ}$ to the midline. Deviating from this angle probably resulted in the severing of the axons leading to the EP, leading to a lack of synaptic responses when the striatum or GP was stimulated.

In vitro electrophysiology. Individual EP neurons were visualized using infrared differential interference contrast microscopy. Electrophysiological recordings were performed in the whole-cell configuration of the patch-clamp technique. Recordings were obtained from the soma of EP neurons using patch pipettes (4–8 M Ω) pulled from thick-walled borosilicate glass capillaries (2.0 mm outer diameter, 0.5 mm wall thickness; Hilgenberg). The standard pipette solution contained the following (in mM): 140 K-gluconate, 10 NaCl, 10 HEPES, 4 MgATP, 0.05 SPERMIN, 5 l-glutathione, 0.2 EGTA, and 0.4 GTP (Sigma-Aldrich), at pH 7.2 with KOH. Under these conditions, the Nernst equilibrium potential for chloride was calculated to be -69.2 mV. The reference electrode was an Ag–AgCl pellet placed in the bath. Voltage and current signals were amplified by an Axopatch-200B amplifier (Molecular Devices), filtered at 5 kHz, and sampled at 20 kHz. Current signals were filtered at 2 kHz and sampled at 20 kHz. The 10 mV liquid junction potential measured under the ionic conditions here was not corrected for. In the voltage-clamp experiments, the pipettes were coated with Sylgard (DOW Corning).

Electrical stimulation was applied via a monopolar 2–3 K Ω Narylene-coated stainless steel microelectrode positioned in the dorsal striatum or GP. The anode was an Ag–AgCl pellet placed in the bath. Stimulation pulses were biphasic 50–500 μ A currents (200 μ s cathodal phase followed by 200 μ s anodal phase). Stimulus trains consisted of 10–20 pulses delivered to the striatum or GP at 1–80 Hz. In several experiments, the following drugs were added to the ACSF: R-SCH23390 to block D₁ type dopamine receptors (final concentration, 10 μ M) and sulpiride to block D₂ type dopamine receptors (final concentration, 3 μ M).

Experimental design and statistical analyses. All off-line analyses were performed using Matlab R2013a (MathWorks; RRID:SCR_001622) and IgorPro 6.0 (WaveMetrics; RRID:SCR_000325) on a personal computer. Data for each experiment were obtained from at least four rats. All results for each experiment were pooled and displayed as the mean \pm SEM, unless mentioned otherwise. The peak amplitude of each synaptic response was calculated after subtraction of the leak current. IPSC latency was calculated as the time from the end of the stimulation to the onset of

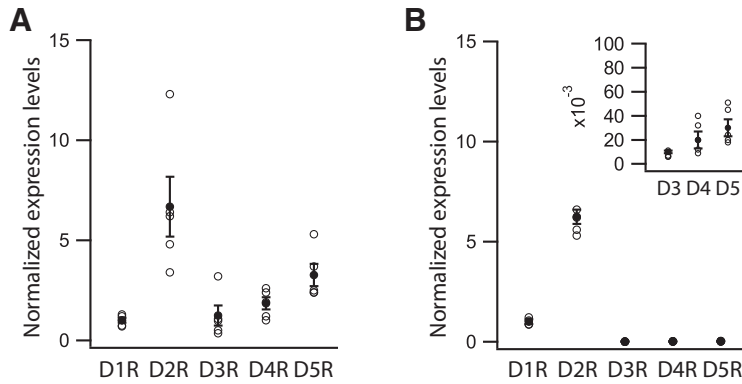


Figure 1. Postsynaptic expression of dopamine receptors in the EP. **A**, Expression levels of dopamine receptor mRNA in the EP, obtained with qRT-PCR ($n = 5$). Expression levels, expressed as the mean \pm SEM, were normalized to the expression levels of D1R. **B**, Expression levels of dopamine receptor mRNA in the striatum, obtained with qRT-PCR ($n = 5$). Inset shows enlarged data for D3R to D5R.

current deflection. Spontaneous firing rate and coefficients of variation (CV) were calculated from recordings that lasted 1–5 min. The prestimulus average firing rate was calculated from spikes extracted from continuous recording of a duration equivalent to that of the stimulation period. Changes in firing pattern were determined through raster plots and changes in spike time entropy throughout the stimulation. A paired t test indicated that the changes in firing rate and entropy between control conditions and after application of dopamine antagonists were significant ($*p < 0.05$ and $**p < 0.01$).

Entropy of spike timing was calculated for each evoked IPSP. The time between two consecutive evoked IPSPs was divided into bins of 10 ms, and the probability of spike discharge was calculated for each bin. Entropy was calculated using the following:

$$H = \sum -\log_2 P * P, \quad (1)$$

and normalized to the maximal entropy value.

Simulating short-term synaptic plasticity in ionotropic synapses. The mathematical framework used here to simulate short-term plasticity was taken from the study by Varela et al. (1997). This model faithfully captures physiological results but deliberately ignores the biological mechanisms underlying short-term plasticity. It is assumed that the post-synaptic amplitude, A , relies on the following three factors: the initial amplitude A_0 , the facilitation variable F , and the depression variable D :

$$A = A_0 F D, \quad (1)$$

Both F and D were initially set to 1.

The depression variable D was multiplied for each stimulus by a constant d representing the depression following a single action potential (AP):

$$D \rightarrow Dd. \quad (2)$$

Since $d \leq 1$, D decreased with each action potential. After each stimulus, D recovered exponentially to 1 using first-order kinetics with a time constant τ_D :

$$\tau_D \frac{dD}{dt} = 1 - D. \quad (3)$$

The facilitation variable F was increased with each stimulus by a constant f representing the facilitation following a single action potential:

$$F \rightarrow F + f, \quad (4)$$

since $f \geq 0$, F increased with each action potential. F increased but was not multiplied by f , since multiplication during high-frequency stimulation caused F to grow beyond all biological proportions. After each stimulus, F recovered exponentially to 1 using first-order kinetics with a time constant τ_F :

$$\tau_F \frac{dF}{dt} = 1 - F. \quad (5)$$

Cellular and synaptic properties. EP neurons were modeled as leaky integrate and fire (LIF) neurons:

$$\frac{dV}{dt} = -\frac{1}{\tau}(V(t) - V_l) + I_{\text{syn}} + I_{\text{noise}}, \quad (6)$$

where V is the neuron membrane potential, τ is the membrane time constant and was set to 10 ms, and I_{syn} is the synaptic current induced by the activity of STR and GP neurons. I_{noise} is a random current injected to induce stochastic spontaneous activity of EP neurons. When the membrane potential V reached -50 mV, an action potential fired and V was reset to -65 mV. Simulated neurons had an average firing rate of 10–15 Hz and a CV of 0.8–1.

We modeled striatum–EP synapses as displaying short-term facilitation. Thus, implementation of these synaptic properties resulted in the following simplification of Equation 1:

$$A = A_0 * F, \quad (7)$$

where $f = 0.6$, $\tau_F = 400$ ms (Hanson and Jaeger, 2002; Lavian and Kornegren, 2015). The initial amplitude of the striatal synapses, A_0 , was set to 10 pA.

Similarly, the GP–EP synapse was modeled to display short-term depression, as follows:

$$A = A_0 * D, \quad (8)$$

where $d = 0.9$, $\tau_D = 1000$ m. The initial amplitude of the pallidal synapses, A_0 , was set to 70 pA.

Results

Dopamine receptors are expressed by EP neurons

Our working hypothesis posited dopaminergic modulation of several EP pathways. To identify these modalities, we first sought to determine the types and distributions of DRs in the EP. For this purpose, we used qRT-PCR to measure DR mRNA levels from small EP tissue samples mechanically extracted from brain slices (Fig. 1A). Our qRT-PCR results detected the mRNA of all DR subtypes, indicating that all the DRs were expressed in the EP. Although all DRs were detected in the EP, the relative expression of the D_2 receptor (D2R) was significantly higher than that of D1R, D3R, D4R, and D5R ($n = 5$; one-way ANOVA, $F_{(4,20)} = 9$, $p < 0.001$; Tukey–Kramer *post hoc* test, $p < 0.05$). To validate our qRT-PCR procedure, we repeated this analysis on tissue samples from the striatum (Fig. 1B) obtaining results identical to the literature (Araki et al., 2007). In the striatum, the expression of D2R was significantly higher than that of D1R, D3R, D4R, and D5R (one-way ANOVA: $F_{(4,20)} = 274$, $p < 0.001$; Tukey–Kramer *post hoc* test: $p < 0.001$), and expression of D1R was significantly higher than that of D3R, D4R, and D5R (Tukey–Kramer *post hoc* test, $p < 0.01$). The detection of mRNA transcripts in the EP suggested postsynaptic expression of all five DRs by EP neurons, supporting the notion of a potent effect of dopamine on EP activity.

Dopamine receptors modulate GABAergic input to EP neurons

Both *in vitro* (Florin et al., 1990) and *in vivo* (Kliem et al., 2007) studies have implicated dopamine in the modulation of GABA

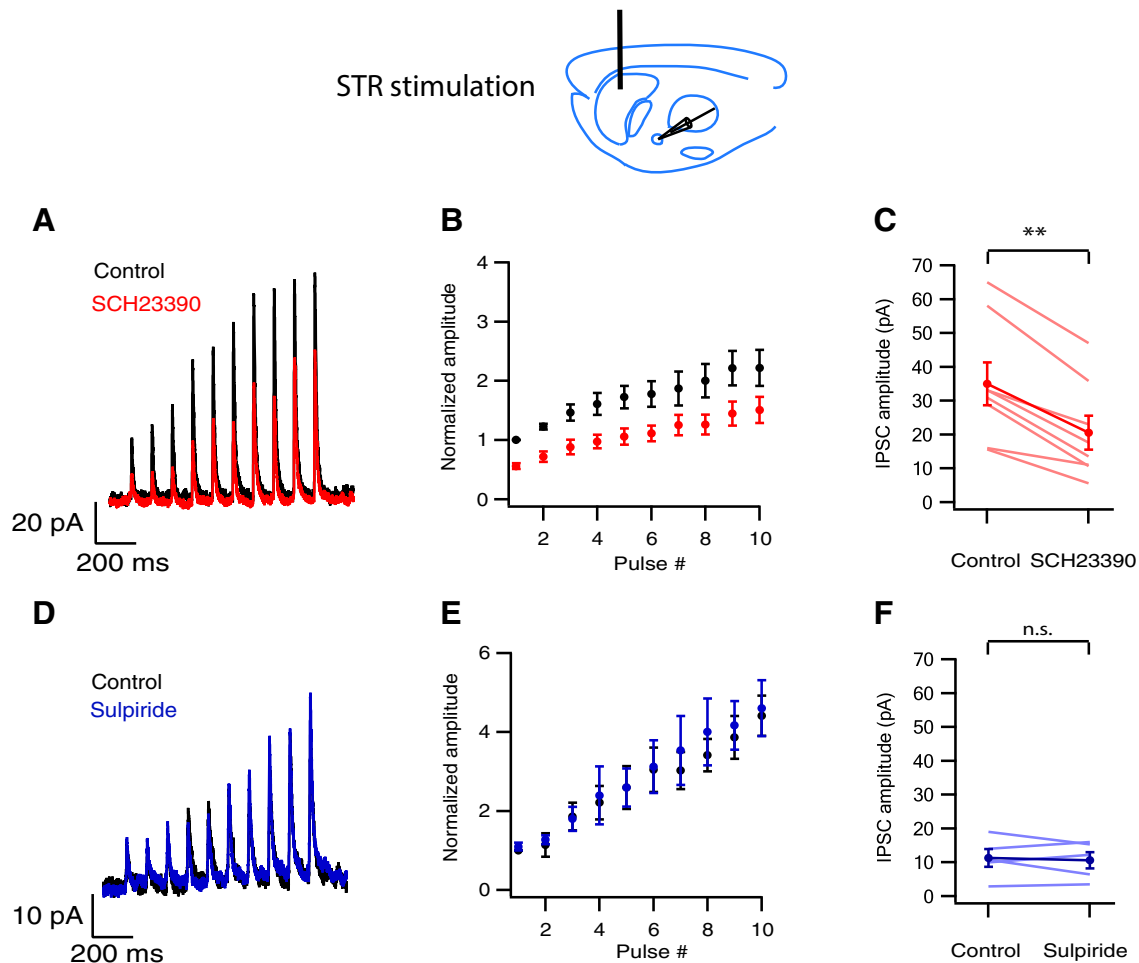


Figure 2. Striatum–EP IPSCs are modulated by D1LR receptors, but not D2LR receptors. **A, D**, Whole-cell voltage-clamp recordings of striatum evoked IPSCs in control conditions (black) and after the application of SCH23390 (**A**, red) or sulpiride (**D**, blue) averaged over 10 consecutive sweeps. **B, E**, Population average of striatum-evoked IPSCs in control conditions and after the application of SCH23390 (**B**, $n = 8$) or sulpiride (**E**, $n = 5$). **C, F**, The amplitude of the first evoked IPSC in the controls and after the application of SCH23390 (**C**) or sulpiride (**F**). Values are given as the mean \pm SEM. * $p < 0.05$, ** $p < 0.01$.

concentration in the EP, suggesting that dopamine could modulate GABAergic synaptic transmission. Furthermore, given the partial symmetry in DR expression levels between the EP and the striatum (Fig. 1), we hypothesized that both D₁-like receptor (D1LR) and D2LR families would influence GABAergic synaptic transmission in the EP. Therefore, we recorded from the somata of EP neurons using the whole-cell configuration of the patch-clamp technique. A train of 10 pulses at 10 Hz delivered to the striatum induced short-term facilitation of the IPSCs, in line with our previous findings (Lavian and Korngreen, 2015; Fig. 2A, B). After the application of D1LR blocker SCH23390, the amplitude of the first IPSC in the train decreased from 35 ± 6 to 20 ± 5 pA ($n = 8$; paired t test, $p < 0.01$; Fig. 2A–C). The application of the D2LR blocker sulpiride did not change the amplitude of the first IPSC (control: 11.3 ± 2.6 pA; sulpiride: 10.6 ± 2.4 pA; paired t test, $p = 0.67$; Fig. 2D–F; $n = 5$). Thus, we concluded, in partial symmetry with the action of dopamine in the striatum, that D1LRs may amplify direct pathway inputs from the striatum to the EP. The paired-pulse ratio (PPR; IPSC2/IPSC1) of striatal evoked IPSCs was not significantly changed by application of SCH23390 (control: 1.22 ± 0.04 ; SCH23390: 1.34 ± 0.13 ; paired t test, $p = 0.3$; $n = 8$). This finding suggests that dopamine modulates striatal synapses via postsynaptic D1LRs.

Next, we investigated the effects of dopamine on GP inputs to the EP. Stimulation of the GP evoked GABAergic IPSCs with a mean amplitude of 59 ± 6 pA ($n = 41$). When the GP was stimulated at 10 Hz, the evoked IPSCs showed short-term depression, which is in line with previous findings (Kita, 2001; Lavian and Korngreen, 2015; Fig. 3A, B). Blocking D1LRs with SCH23390 did not change the amplitude of the first IPSC in the train (control: 62.5 ± 17.9 pA; SCH23390: 62.2 ± 19.4 pA; paired t test, $p = 0.95$; Fig. 3A–C). However, blocking D2LRs with sulpiride increased IPSCs from 65 ± 9 to 90 ± 12 pA ($n = 19$; paired t test, $p < 0.001$; Fig. 3D–F). Hence, D2LRs appeared to depress indirect pathway inputs from the GP to the EP. Moreover, the PPR of GP-evoked IPSCs was significantly decreased by the application of sulpiride (control: 0.68 ± 0.02 ; sulpiride: 0.6 ± 0.02 ; paired t test, $p = 0.002$; $n = 19$). This decrease in PPR suggests that dopamine acts presynaptically on pallidal synapses in the EP via D2LRs.

Dopamine receptors modulate firing of EP neurons

Theoretical studies have suggested that short-term synaptic plasticity plays a role in optimizing information transmission (Rotman et al., 2011). We showed previously that GABAergic transmission affects the firing of EP neurons (Lavian and Korn-

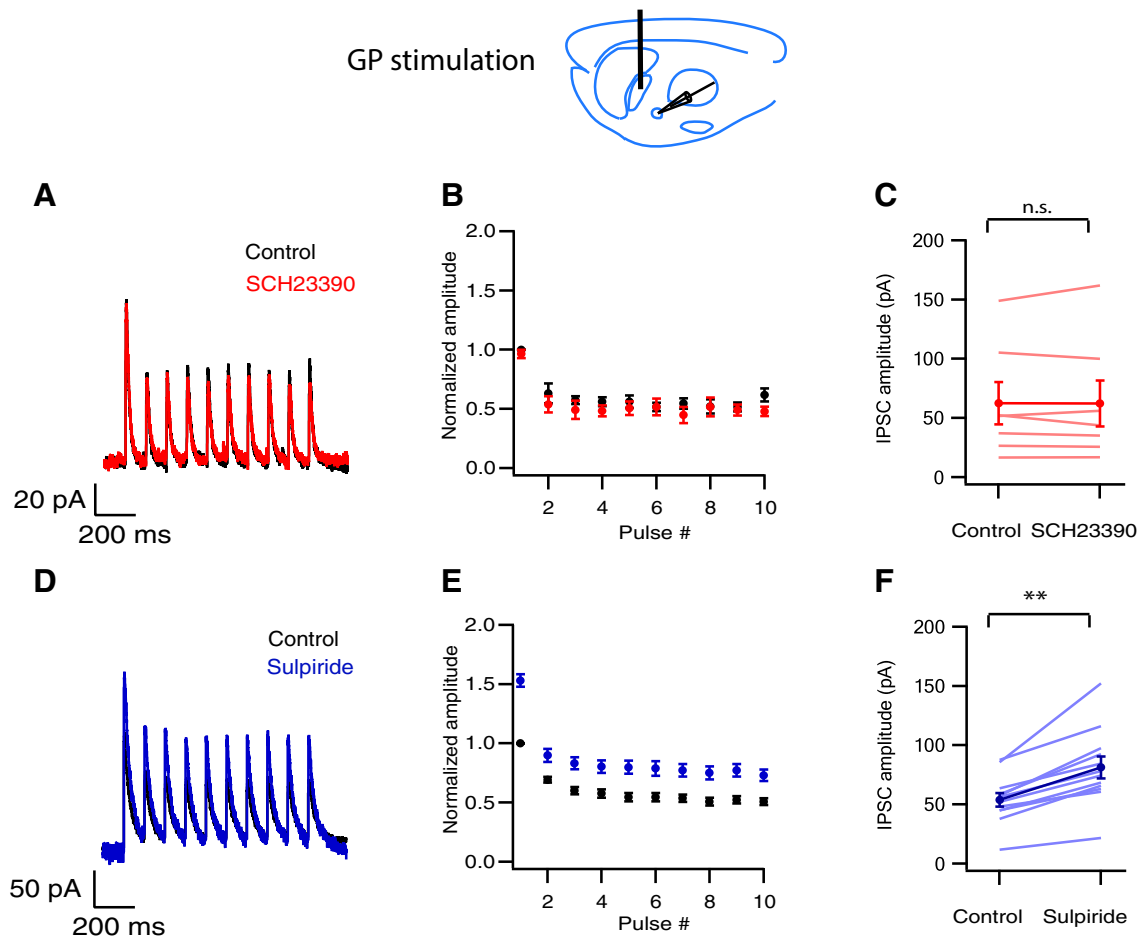


Figure 3. GP–EP IPSCs are modulated by D2LR receptors, but not D1LR receptors. **A, D**, Whole-cell voltage-clamp recordings of GP-evoked IPSCs in control conditions (black) and after application of SCH23390 (**A**, red) or sulpiride (**D**, blue) averaged over 10 consecutive sweeps. **B, E**, Population average of GP-evoked IPSCs in control conditions and after the application of SCH23390 (**B**, $n = 7$) or sulpiride (**E**, $n = 19$). **C, F**, The amplitude of the first evoked IPSC in the controls and after application of SCH23390 (**C**) or sulpiride (**F**). Values are given as the mean \pm SEM. * $p < 0.05$, ** $p < 0.01$.

green, 2015). Thus, we hypothesized that dopaminergic modulation of GABAergic input would also impact EP firing. We recorded the responses of individual spontaneously firing neurons in the EP to repetitive stimulation of the striatum in the current-clamp mode (Fig. 4*A, B*). Stimulation at 10 or 20 Hz induced a continuous decrease in firing rate (Fig. 4*C*) and a decrease in spike-timing entropy that increased with each IPSP (Fig. 4*D*). A decrease in spike time entropy may suggest that the firing of the postsynaptic neuron can become more predictable but may also stem from the decrease in firing rate. To determine the source of the changes in entropy, we measured the latency of the spike discharge from each evoked IPSP and calculated the mean and SD of the latency across trials (Fig. 4*E*). We found that each evoked IPSP induced a greater delay in spike discharge latency, as well as a greater decrease in the latency SD, suggesting that the timing of the spike discharge became more precise. Blocking D1LR with SCH23390 partially blocked the progressive decrease in firing rate (20 Hz stimulation: $70 \pm 2\%$ of baseline compared with $48 \pm 6\%$ of baseline, $n = 9$, paired t test, $p < 0.001$; Fig. 4*C*). Changes in entropy were also dopamine dependent, since under control conditions the maximal decrease in spike time entropy was to $42 \pm 4\%$ of the baseline, whereas after application of SCH23390 it was only $68 \pm 10\%$ of the baseline ($n = 9$; paired t test, $p < 0.001$; Fig. 4*D*). Thus, blocking D1LR apparently decreased the ability of GABAergic input from the striatum to mod-

ulate activity in the EP. The firing of EP neurons in acute brain slices is semiregular whereas *in vivo* it is more stochastic. Thus, the increase in firing rate and entropy could have been due to a slice artifact. We used simple numerical modeling to negate this possibility. Using a random fluctuating current, we drove a LIF neuron (Eq. 6), inducing it to fire a stochastic spike train (CV between 0.8 and 1). We then repeatedly stimulated a model of a facilitating GABAergic synapse (Eq. 7) connected to this neuron. We did not fit the model to the experimental spike trains but, rather, only adjusted the initial IPSC amplitude to approximately the same one observed experimentally. Our simulations showed that a facilitating inhibitory synapse can induce a continuous decrease in the spike time entropy of Poisson neurons, indicating that our findings are applicable to more realistic neuronal activity (Fig. 6*A–D*).

We further investigated the effect of D2LRs on the effect of pallidal GABAergic inputs to the EP (Fig. 5*A, B*). During stimulation of the GP at 20 Hz, there was a significant decrease in firing rate and spike time entropy of EP neurons (Fig. 5*C–E*). We found that the first evoked IPSP induced a strong transient decrease in firing rate and spike time entropy, whereas the effect of the following IPSPs was smaller. These effects on EP firing were reproducible in our LIF simulations (Fig. 6*E–H*). After application of sulpiride, the maximal decrease in firing rate was $39 \pm 12\%$ of the baseline, which was significantly larger than the control ($n = 5$;

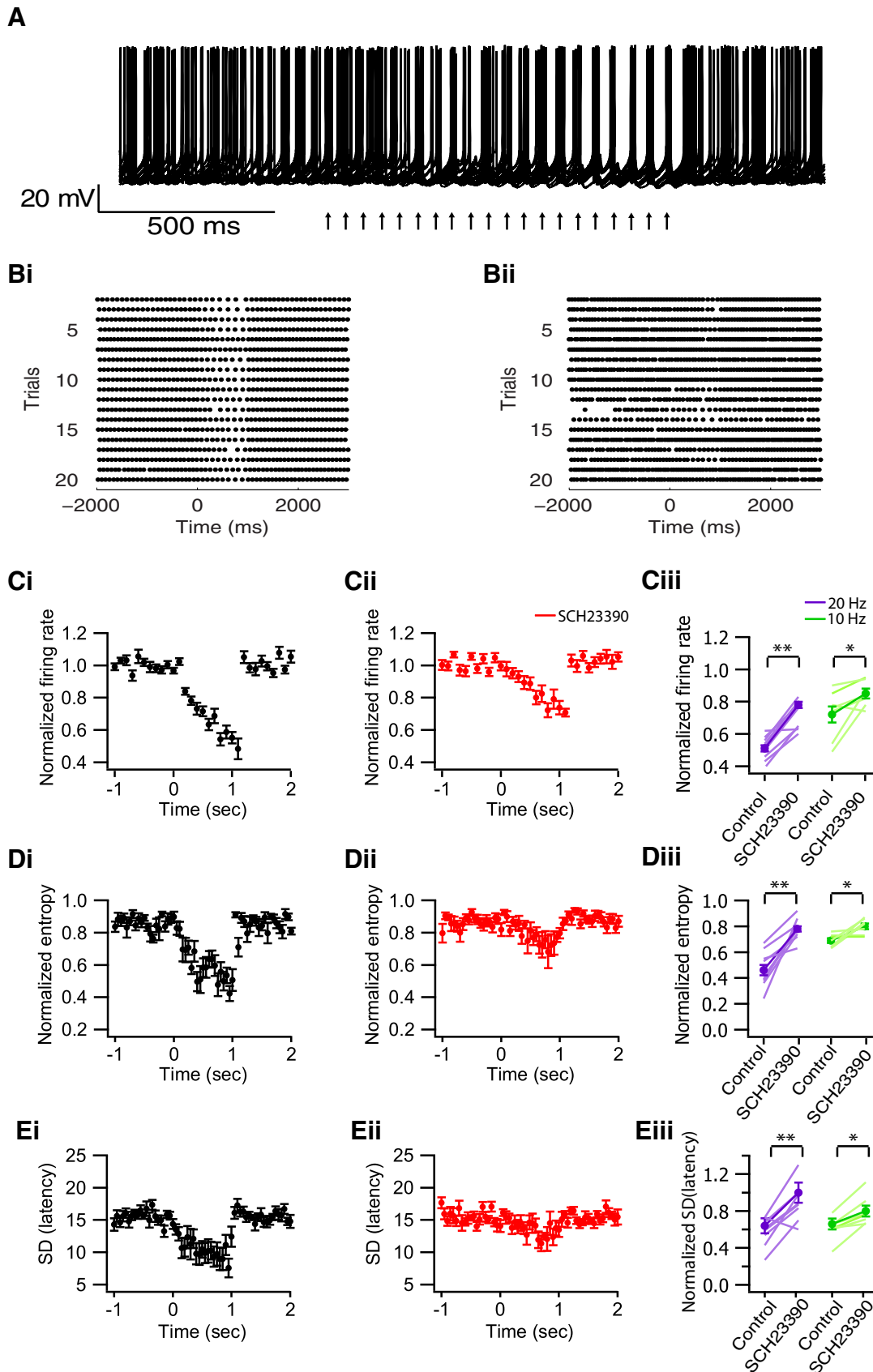


Figure 4. Striatal inputs induce a continuous decrease in spike time entropy of EP neurons in a dopamine-dependent manner. **A**, Effects of repetitive activation of striatal synapses on the firing pattern in the EP. Repetitive stimulation of the striatum at 20 Hz, where arrows indicate the timing of stimulation pulses. In this and all subsequent recordings, stimulation artifacts were removed for clarity. Ten sweeps were overlaid to more clearly show the effect of the stimulations. **Bi, Bii**, Raster plots of the response of an EP neuron to 20 Hz stimulation of the striatum in control conditions (**Bi**) and after application of SCH23390 (**Bii**). **Ci, Cii**, Changes in firings rate induced by 20 Hz stimulation of the striatum in control conditions (**Ci**) and after (Figure legend continues.)

paired *t* test, $p < 0.05$; Fig. 5C). Moreover, in control conditions the decrease in spike time entropy following the first IPSP was $34 \pm 11\%$ of the baseline, and after application of sulpiride it was $10 \pm 9\%$ of the baseline ($n = 5$; paired *t* test, $p < 0.05$; Fig. 5D). We also measured the latency of the spike discharge from each evoked IPSP and calculated the mean and SD of the latency across trials (Fig. 5E). We found that the first evoked IPSP induced a greater delay in spike discharge as well as a greater decrease in latency SD. Together, our experiments suggest that dopaminergic input facilitates the passage of information reaching the EP via the direct pathway while it concurrently depresses information reaching the EP through the indirect pathway.

Discussion

Here we showed that all DR subtypes are expressed in the EP, that GABAergic synapses in the direct and indirect pathways are differentially modulated by D1LRs and D2LRs receptors respectively in a manner reflecting their processing in the striatum, and that these GABAergic synapses can decrease the spike time entropy of EP neurons in a dopamine-dependent manner. Our findings suggest that dopamine regulates the balance between the inputs of the direct and indirect pathways in the EP, thus forming an output amplifier for motor or limbic programs propagating through the basal ganglia.

Because dopamine is critical for the normal functioning of the basal ganglia, and in light of the evidence for dopaminergic modulation of activity in the EP (DeLong, 1990; Filion and Tremblay, 1991; Ruskin et al., 2002; Darbin et al., 2016), we investigated how dopamine shapes the activity of neurons in the EP. We used qRT-PCR to show that all dopamine receptors are expressed in the EP (Fig. 1). These results are in partial agreement with previous studies observing D1R (Yung et al., 1995), D4R (Rivera et al., 2003), and D5R (Ciliax et al., 2000) in the EP. However, there is conflicting evidence regarding the expression of D2R; whereas one study did not detect D2R in rats (Yung et al., 1995), others have detected small amounts of D2R in the EP of rats (Boyson et al., 1986) and cats (Beckstead et al., 1988). This discrepancy may be due to the improved sensitivity of qRT-PCR compared with earlier methods.

Dopamine receptors modulate synaptic transmission in the EP

Here we show that dopamine modulates GABAergic inputs in the EP, similar to its effects in another basal ganglia output nucleus, the SNr (de Jesús Aceves et al., 2011; Figs. 2, 3). Previous studies have shown that dopamine can alter the GABA concentration in these two nuclei (Floran et al., 1990; Aceves et al., 1995) and have suggested that this effect is mediated by presynaptic dopamine receptors expressed on GABAergic axons originating in the striatum and GP. Our results show that indeed dopamine modulates the GABAergic inputs from striatum and GP in the EP.

The neurons in the EP and SNr share many electrophysiological and anatomical properties. In both nuclei, GP synapses are somatic and show short-term depression, whereas striatal synapses are located on distal dendrites and show short-term facilitation (Smith and Bolam, 1991; Bolam and Smith, 1992; Kita, 2001; Connelly et al., 2010). Moreover, in the two nuclei these synapses are modulated by dopamine (de Jesús Aceves et al., 2011), suggesting that our findings might be applicable to the SNr as well. However, here we found that the PPR of striatal evoked IPSCs in the EP was not changed by the application of SCH23390, suggesting a postsynaptic mechanism, which is different from the findings of a previous study that found that in the SNr, the PPR of striatal evoked IPSCs increases in the presence of SCH23390, which may imply a presynaptic mechanism (de Jesús Aceves et al., 2011). Moreover, the dopaminergic neurons of the SNc are closer to the SNr, and SNc dendrites invade the SNr where they release dopamine (Geffen et al., 1976; Cheramy et al., 1981). Thus, whereas the short-term plasticity of GABAergic synapses in the SNr is similar to that of the EP, dopaminergic modulation of these synapses is probably different.

The EP consists of several neuronal types, which differ in terms of their biochemistry, location along the EP, afferents, and target nuclei (Kha et al., 2000; Wallace et al., 2017). In the present study, we did not attempt to classify the neurons we investigated. Our electrophysiological recordings were collected from neurons all over the EP. Our electrophysiological analysis did not reveal any heterogeneity: all striatum-evoked IPSCs and all GP-evoked IPSCs were modulated similarly by the application of D1LR and D2LR antagonists. This possible homogenous innervation pattern is consistent with a recent elegant study demonstrating that different cell types in the EP receive similar GABAergic input from the striatum and GP (Wallace et al., 2017).

Dopamine redistributes information between the direct and indirect pathways in the EP

Theory suggests that synaptic plasticity plays a role in optimizing information transmission (Rotman et al., 2011). Here we investigated two types of GABAergic synapses that exhibit different forms of synaptic plasticity and showed that these synapses have different effects on postsynaptic firing patterns. The facilitating synapses from the striatum induced a continuous decrease in spike time entropy that increased with each presynaptic AP, indicating that bursts of striatal APs can modulate EP firing, hence increasing its predictability. We further showed that the ability of striatal projection neurons to modulate firing in the EP is dopamine dependent (Fig. 4). These results are in line with those of a recent study showing that dopamine depletion induces an increase in the entropy rate of EP neurons (Darbin et al., 2016).

The effects of the depressing synapses from the GP on EP firing differed from those of the striatal synapses. As these synapses depress, they function as a low-pass filter (Chance et al., 1998; Fortune and Rose, 2001). Our findings suggest that when a GP neuron fires a series of APs, the first AP induces a greater delay in the spike discharge than the delay induced by the subsequent APs. Moreover, we showed that the first evoked IPSP induces a transient drop in spike time entropy, whereas the next IPSPs have a lesser effect, which coincides with the ability of single GP stimulation to synchronize EP neurons (Kita, 2001). Our results may indicate that dopamine can reduce this ability of GP neurons (Fig. 5).

←

(Figure legend continued.) application of SCH23390 (Cii; $n = 9$). Ciii, Normalized firing rate at the time of the last IPSC evoked by 10 or 20 Hz stimulation in the controls and after application of SCH23390. Di, Dii, changes in spike time entropy induced by 20 Hz stimulation of the striatum in the control conditions (Di) and after application of SCH23390 (Dii; $n = 9$). Diii, Normalized entropy at the time of the last evoked IPSC in the controls and after application of SCH23390. Ei, Eii, Changes in the SD of the latency of spike discharge induced by each evoked IPSP calculated for 20 Hz stimulation of the striatum in control conditions (Ei) and after the application of SCH23390 (Eii; $n = 6$). Eiii, Normalized change in the SD of the latency at the time of the last evoked IPSC in control and after application of SCH23390. Values are given as the mean \pm SEM. ** $p < 0.001$, * $p < 0.05$.

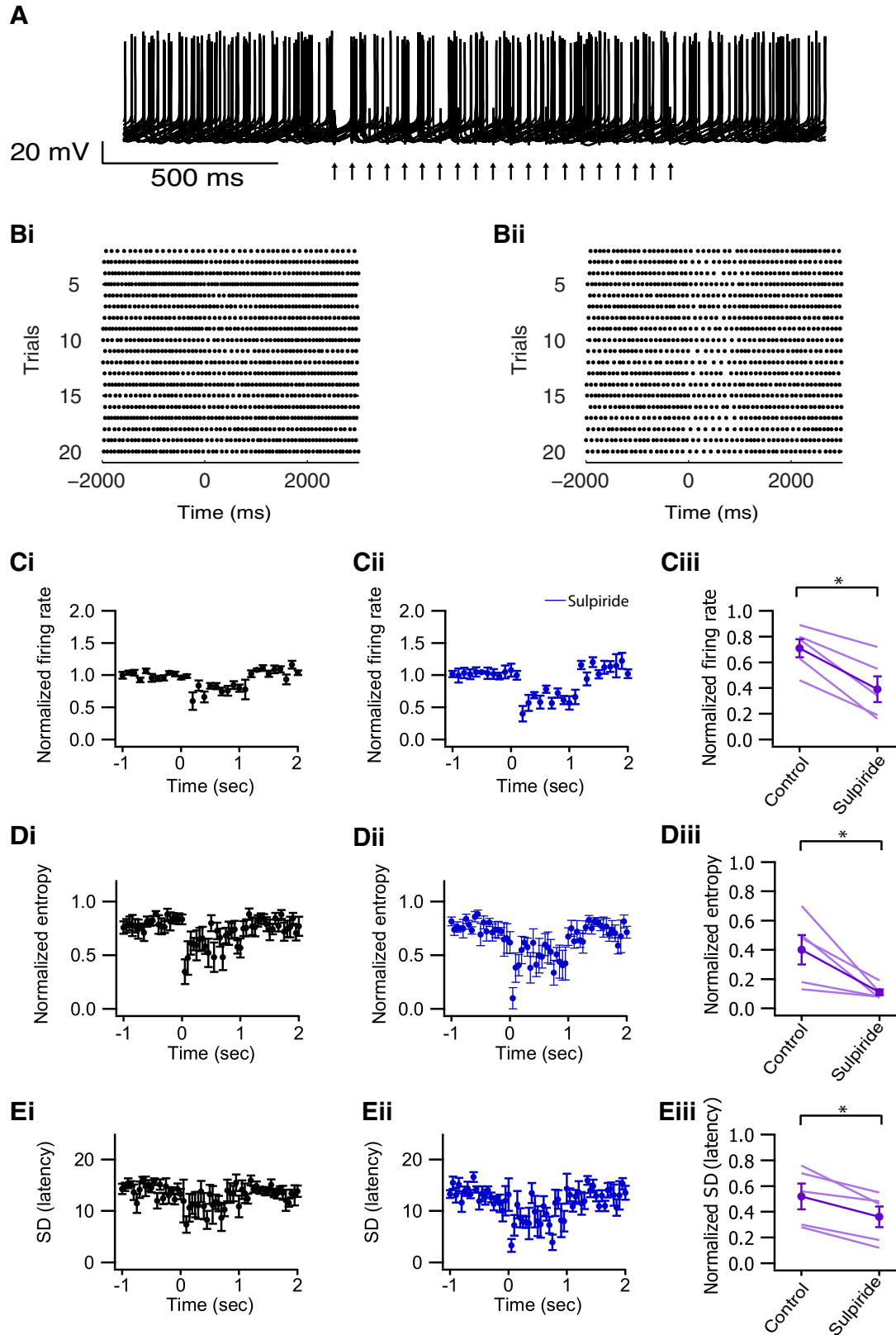


Figure 5. GP inputs induce a transient decrease in spike time entropy of EP neurons in a dopamine-dependent manner. **A**, Repetitive stimulation of the GP at 20 Hz, arrows indicate timing of stimulation pulses. Ten sweeps were overlaid to more clearly show the effect of the stimulations on the spontaneous activity. **Bi, Bii**, Raster plots of the response of an EP neuron to 20 Hz stimulation of the GP in control conditions (**Bi**) and after application of sulpiride (**Bii**). **Ci, Cii**, Changes in firings rate induced by 20 Hz stimulation of the GP in control conditions (**Ci**) and after application of sulpiride (**Cii**; $n = 5$). **Ciii**, Normalized firing rate at the time of the first evoked IPSC in control and after application of sulpiride. **Di, Dii**, Changes in spike time entropy induced by 20 Hz stimulation of the GP in control conditions (**Di**) and after application of sulpiride (**Dii**; $n = 5$). **Diii**, Normalized entropy at the time of the first evoked IPSC in control and after application of sulpiride. **Ei, Eii**, Changes in the SD of the latency of spike discharge induced by each evoked IPSP calculated for 20 Hz stimulation of the GP in control conditions (**Ei**) and after application of sulpiride (**Eii**; $n = 6$). Values are given as the mean \pm SEM. * $p < 0.05$.

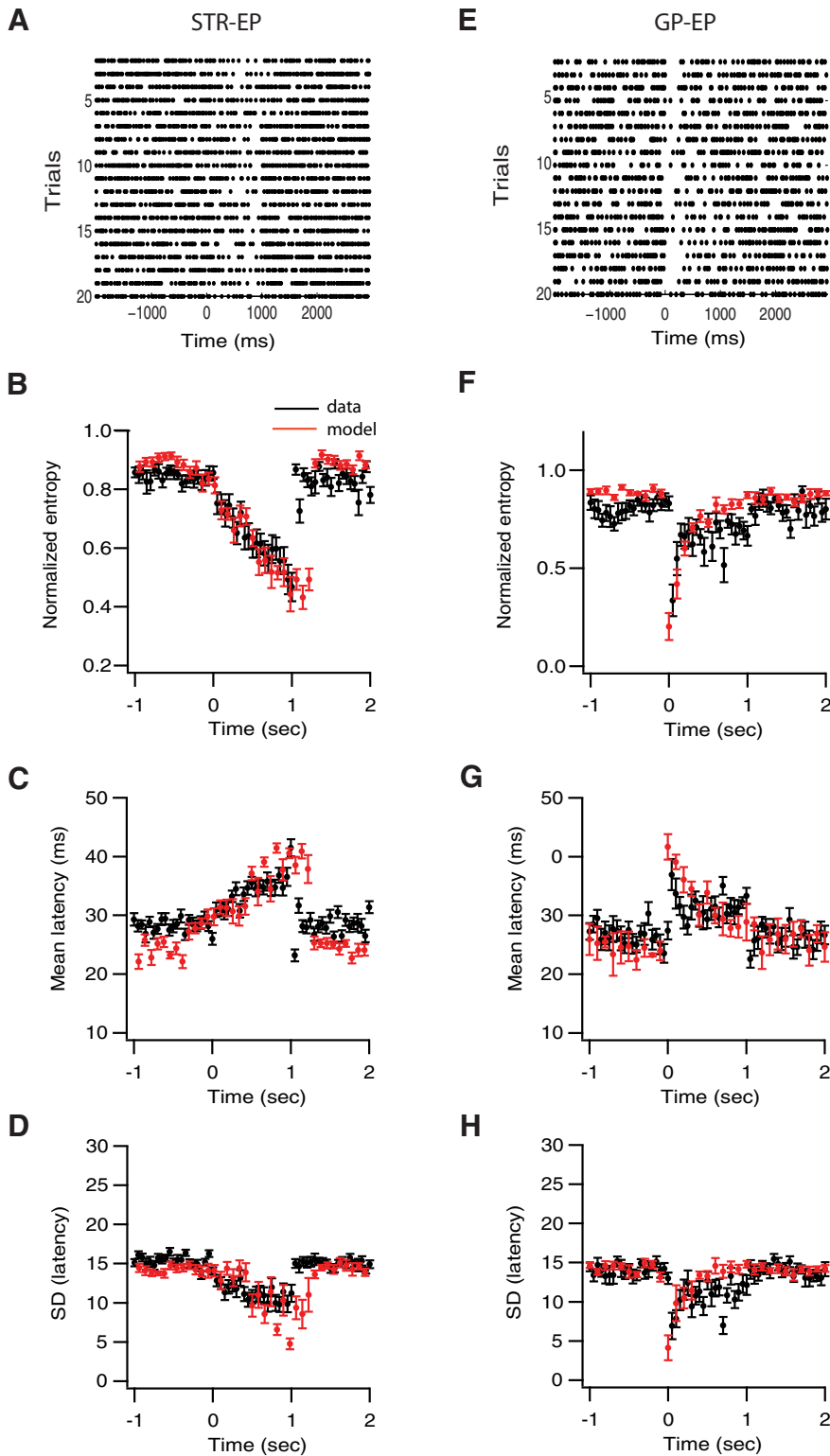


Figure 6. Simulated data show that striatum and GP inputs can modulate the firing of Poisson neurons. *A, E*, Raster plots of the response of a simulated Poisson neuron to 20 Hz stimulation of the striatum (*A*) and the GP (*E*). *B, F*, Changes in spike time entropy induced by 20 Hz stimulation of the striatum (*B*) and the GP (*F*; $n = 10$). *C, G*, Changes in average latency of spike discharge induced by each evoked IPSP calculated for 20 Hz stimulation of the striatum (*C*) and the GP (*G*; $n = 10$). *D, H*, Changes in the SD of the latency of spike discharge induced by each evoked IPSP calculated for 20 Hz stimulation of the striatum (*D*) and the GP (*H*; $n = 10$). In all panels, the experimental data are presented with black symbols and LIF stimulation is presented with red symbols. The results of the simulation were not fitted to the data; they were overlaid on the experiments to allow for qualitative comparison. Values are given as the mean \pm SEM.

The basal ganglia have long been implicated in motor control and action selection (Albin et al., 1989; DeLong, 1990). Recently, it has been claimed that both the direct and indirect pathways of the basal ganglia are necessary for action initiation and execution (Tecuapetla et al., 2016). Moreover, in the EP, the point of integration of these two pathways (Nagy et al., 1978; Bolam and Smith, 1992), dopamine-mediated transmission is necessary to release movement. We posit a possible mechanism for the gating of motor programs by dopamine. Cortical information briefly activates striatal SPNs. Activated SPNs can temporally decrease the entropy of EP neurons and lock their firing pattern to that of their own. The larger the facilitation of the striatal–EP synapse, the stronger the phase lock will be. This predicts a correlation between an EP neuron and the SPN innervating it following cortical activation. This increase in mutual information should be manifested by a reduction in spike train entropy. Thus, reduction of entropy may be viewed as an indicator of the passage of information from the striatum via the EP. Concurrently with this flow of information from the striatum, short-term depression of perisomatic synapses from the GP may reduce the inhibition of the flow of striatal information. Release of dopamine in the EP would thus alter this dynamic balance between the striatum and GP in which striatal synapses potentiate while pallidal synapses depress, enhancing information flow from the striatum to the thalamus and other targets outside the basal ganglia. Conversely, when dopaminergic signaling is impaired, the ability of SPNs to control EP firing should be reduced, hence limiting the transmission of motor programs from the basal ganglia to the thalamus and other brain regions. Thus, our results may hint that short-term plasticity in EP neurons actively multiplexes information in the direct and indirect pathways of the basal ganglia. Furthermore, during processes such as action selection and learning, which are facilitated by dopamine release, information from the striatum may be given dominance over that from the GP in single EP neurons. Together, these findings could imply that dopamine concurrently controls both the separation of cortical input to the basal ganglia in the striatum and the recombination of this information downstream in the EP, which would act as a global modulator of the feedforward network of the basal ganglia.

References

- Aceves J, Floran B, Sierra A, Mariscal S (1995) D-1 receptor mediated modulation of the release of gamma-aminobutyric acid by endogenous dopamine in the basal ganglia of the rat. *Prog Neuropsychopharmacol Biol Psychiatry* 19:727–739. [CrossRef Medline](#)
- Albin RL, Young AB, Penney JB (1989) The functional anatomy of basal ganglia disorders. *Trends Neurosci* 12:366–375. [CrossRef Medline](#)
- Araki KY, Sims JR, Bhide PG (2007) Dopamine receptor mRNA and protein expression in the mouse corpus striatum and cerebral cortex during pre- and postnatal development. *Brain Res* 1156:31–45. [CrossRef Medline](#)
- Bar-Gad I, Havazelet-Heimer G, Goldberg JA, Ruppin E, Bergman H (2000) Reinforcement-driven dimensionality reduction—a model for information processing in the basal ganglia. *J Basic Clin Physiol Pharmacol* 11:305–320. [Medline](#)
- Beckstead RM, Domesick VB, Nauta WJ (1979) Efferent connections of the substantia nigra and ventral tegmental area in the rat. *Brain Res* 175:191–217. [CrossRef Medline](#)
- Beckstead RM, Wooten GF, Trugman JM (1988) Distribution of D1 and D2 dopamine receptors in the basal ganglia of the cat determined by quantitative autoradiography. *J Comp Neurol* 268:131–145. [CrossRef Medline](#)
- Beninger RJ (1983) The role of dopamine in locomotor activity and learning. *Brain Res* 287:173–196. [Medline](#)
- Bergman H, Feingold A, Nini A, Raz A, Sloviter H, Abeles M, Vaadia E (1998) Physiological aspects of information processing in the basal ganglia of normal and parkinsonian primates. *Trends Neurosci* 21:32–38. [CrossRef Medline](#)
- Bolam JP, Smith Y (1992) The striatum and the globus pallidus send convergent synaptic inputs onto single cells in the entopeduncular nucleus of the rat: a double anterograde labelling study combined with postembedding immunocytochemistry for GABA. *J Comp Neurol* 321:456–476. [CrossRef Medline](#)
- Bolam JP, Hanley JJ, Booth PA, Bevan MD (2000) Synaptic organisation of the basal ganglia. *J Anat* 196:527–542. [CrossRef Medline](#)
- Boyson SJ, McGonigle P, Molinoff PB (1986) Quantitative autoradiographic localization of the D1 and D2 subtypes of dopamine receptors in rat brain. *J Neurosci* 6:3177–3188. [Medline](#)
- Caillé I, Dumartin B, Bloch B (1996) Ultrastructural localization of D1 dopamine receptor immunoreactivity in rat striatonigral neurons and its relation with dopaminergic innervation. *Brain Res* 730:17–31. [CrossRef Medline](#)
- Chance FS, Nelson SB, Abbott LF (1998) Synaptic depression and the temporal response characteristics of V1 cells. *J Neurosci* 18:4785–4799. [Medline](#)
- Cheramy A, Levil V, Glowinski J (1981) Dendritic release of dopamine in the substantia nigra. *Nature* 289:537–542. [CrossRef Medline](#)
- Ciliax BJ, Nash N, Heilman C, Sunahara R, Hartney A, Tiberi M, Rye DB, Caron MG, Niznik HB, Levey AI (2000) Dopamine D(5) receptor immunolocalization in rat and monkey brain. *Synapse* 37:125–145. [CrossRef Medline](#)
- Connelly WM, Schulz JM, Lees G, Reynolds JN (2010) Differential short-term plasticity at convergent inhibitory synapses to the substantia nigra pars reticulata. *J Neurosci* 30:14854–14861. [CrossRef Medline](#)
- Darbin O, Jin X, Von Wrangel C, Schwabe K, Nambu A, Naritoku DK, Krauss JK, Alam M (2016) Neuronal entropy-rate feature of entopeduncular nucleus in rat model of Parkinson's disease. *Int J Neural Syst* 26:1550038. [CrossRef Medline](#)
- de Jesús Aceves J, Rueda-Orozco PE, Hernández R, Plata V, Ibañez-Sandoval O, Galarraga E, Vargas J (2011) Dopaminergic presynaptic modulation of nigral afferents: its role in the generation of recurrent bursting in substantia nigra pars reticulata neurons. *Front Syst Neurosci* 5:6. [CrossRef Medline](#)
- DeLong MR (1990) Primate models of movement disorders of basal ganglia origin. *Trends Neurosci* 13:281–285. [CrossRef Medline](#)
- Filion M, Tremblay L (1991) Abnormal spontaneous activity of globus pallidus neurons in monkeys with MPTP-induced parkinsonism. *Brain Res* 547:142–151. [Medline](#)
- Floran B, Aceves J, Sierra A, Martinez-Fong D (1990) Activation of D1 dopamine receptors stimulates the release of GABA in the basal ganglia of the rat. *Neurosci Lett* 116:136–140. [CrossRef Medline](#)
- Fortune ES, Rose GJ (2001) Short-term synaptic plasticity as a temporal filter. *Trends Neurosci* 24:381–385. [CrossRef Medline](#)
- Fuchs H, Hauber W (2004) Dopaminergic innervation of the rat globus pallidus characterized by microdialysis and immunohistochemistry. *Exp Brain Res* 154:66–75. [CrossRef Medline](#)
- Gauthier J, Parent M, Lévesque M, Parent A (1999) The axonal arborization of single nigrostriatal neurons in rats. *Brain Res* 834:228–232. [CrossRef Medline](#)
- Geffen LB, Jessell TM, Cuello AC, Iversen LL (1976) Release of dopamine from dendrites in rat substantia nigra. *Nature* 260:258–260. [CrossRef Medline](#)
- Gerfen CR, Surmeier DJ (2011) Modulation of striatal projection systems by dopamine. *Annu Rev Neurosci* 34:441–466. [CrossRef Medline](#)
- Hanson JE, Jaeger D (2002) Short-term plasticity shapes the response to simulated normal and parkinsonian input patterns in the globus pallidus. *J Neurosci* 22:5164–5172. [Medline](#)
- Kha HT, Finkelstein DI, Pow DV, Lawrence AJ, Horne MK (2000) Study of projections from the entopeduncular nucleus to the thalamus of the rat. *J Comp Neurol* 426:366–377. [CrossRef Medline](#)
- Kita H (2001) Neostriatal and globus pallidus stimulation induced inhibitory postsynaptic potentials in entopeduncular neurons in rat brain slice preparations. *Neuroscience* 105:871–879. [CrossRef Medline](#)
- Kliem MA, Maidment NT, Ackerson LC, Chen S, Smith Y, Wichmann T (2007) Activation of nigral and pallidal dopamine D1-like receptors modulates basal ganglia outflow in monkeys. *J Neurophysiol* 98:1489–1500. [CrossRef Medline](#)
- Kliem MA, Pare JF, Khan ZU, Wichmann T, Smith Y (2010) Ultrastructural localization and function of dopamine D1-like receptors in the substantia nigra pars reticulata and the internal segment of the globus pallidus of parkinsonian monkeys. *Eur J Neurosci* 31:836–851. [CrossRef Medline](#)
- Lavian H, Korngreen A (2016) Inhibitory short-term plasticity modulates neuronal activity in the rat entopeduncular nucleus in vitro. *Eur J Neurosci* 43:870–884. [CrossRef Medline](#)
- Lavian H, Ben-Porat H, Korngreen A (2013) High and low frequency stimulation of the subthalamic nucleus induce prolonged changes in subthalamic and globus pallidus neurons. *Front Syst Neurosci* 7:73. [CrossRef Medline](#)
- Lindvall O, Björklund A, Moore RY, Stenevi U (1974) Mesencephalic dopamine neurons projecting to neocortex. *Brain Res* 81:325–331. [CrossRef Medline](#)
- Mitkovski M, Padovan-Neto FE, Raisman-Vozari R, Ginestet L, da-Silva CA, Del-Bel EA (2012) Investigations into potential extrasynaptic communication between the dopaminergic and nitroergic systems. *Front Physiol* 3:372. [CrossRef Medline](#)
- Nagy JJ, Carter DA, Fibiger HC (1978) Anterior striatal projections to the globus pallidus, entopeduncular nucleus and substantia nigra in the rat: the GABA connection. *Brain Res* 158:15–29. [CrossRef Medline](#)
- Nakahara H, Itoh H, Kawagoe R, Takikawa Y, Hikosaka O (2004) Dopamine neurons can represent context-dependent prediction error. *Neuron* 41:269–280. [CrossRef Medline](#)
- Oorschot DE (1996) Total number of neurons in the neostriatal, pallidal, subthalamic, and substantia nigral nuclei of the rat basal ganglia: a stereological study using the cavalieri and optical disector methods. *J Comp Neurol* 366:580–599. [CrossRef Medline](#)
- Rivera A, Trias S, Peñafiel A, Angel Narváez J, Díaz-Cabiale Z, Moratalla R, de la Calle A (2003) Expression of D4 dopamine receptors in striatonigral and striatopallidal neurons in the rat striatum. *Brain Res* 989:35–41. [CrossRef Medline](#)
- Rommelfanger KS, Wichmann T (2010) Extrastriatal dopaminergic circuits of the basal ganglia. *Front Neuroanat* 4:139. [CrossRef Medline](#)
- Rotman Z, Deng PY, Klyachko VA (2011) Short-term plasticity optimizes synaptic information transmission. *J Neurosci* 31:14800–14809. [CrossRef Medline](#)
- Ruskin DN, Bergstrom DA, Walters JR (2002) Nigrostriatal lesion and dopamine agonists affect firing patterns of rodent entopeduncular nucleus neurons. *J Neurophysiol* 88:487–496. [CrossRef Medline](#)
- Schultz W, Apicella P, Scarnati E, Ljungberg T (1992) Neuronal activity in monkey ventral striatum related to the expectation of reward. *J Neurosci* 12:4595–4610. [Medline](#)
- Smith Y, Bolam JP (1991) Convergence of synaptic inputs from the striatum and the globus pallidus onto identified nigrocollicular cells in the rat: a double anterograde labelling study. *Neuroscience* 44:45–73. [CrossRef Medline](#)
- Smith Y, Lavoie B, Dumas J, Parent A (1989) Evidence for a distinct nigro-

- pallidal dopaminergic projection in the squirrel monkey. *Brain Res* 482:381–386. [CrossRef Medline](#)
- Stuart GJ, Dodt HU, Sakmann B (1993) Patch-clamp recordings from the soma and dendrites of neurons in brain slices using infrared video microscopy. *Pflugers Arch* 423:511–518. [CrossRef Medline](#)
- Tecuapetla F, Jin X, Lima SQ, Costa RM (2016) Complementary contributions of striatal projection pathways to action initiation and execution. *Cell* 166:703–715. [CrossRef Medline](#)
- Varela JA, Sen K, Gibson J, Fost J, Abbott LF, Nelson SB (1997) A quantitative description of short-term plasticity at excitatory synapses in layer 2/3 of rat primary visual cortex. *J Neurosci* 17:7926–7940. [Medline](#)
- Wallace ML, Saunders A, Huang KW, Philson AC, Goldman M, Macosko EZ, McCarroll SA, Sabatini BL (2017) Genetically distinct parallel pathways in the entopeduncular nucleus for limbic and sensorimotor output of the basal ganglia. *Neuron* 94:138–152.e5. [CrossRef Medline](#)
- Watabe-Uchida M, Zhu L, Ogawa SK, Vamanrao A, Uchida N (2012) Whole-brain mapping of direct inputs to midbrain dopamine neurons. *Neuron* 74:858–873. [CrossRef Medline](#)
- Wickens JR, Horvitz JC, Costa RM, Killcross S (2007) Dopaminergic mechanisms in actions and habits. *J Neurosci* 27:8181–8183. [CrossRef Medline](#)
- Yung KK, Bolam JP, Smith AD, Hersch SM, Ciliax BJ, Levey AI (1995) Immunocytochemical localization of D1 and D2 dopamine receptors in the basal ganglia of the rat: light and electron microscopy. *Neuroscience* 65:709–730. [CrossRef Medline](#)